Optical Materials: X 17 (2023) 100219

Contents lists available at ScienceDirect

Optical Materials: X

journal homepage: www.journals.elsevier.com/optical-materials-x

(INVITED) Bi-doped optical fibers and fiber amplifiers

Yu Wang *, Siyi Wang, Arindam Halder, Jayanta Sahu **

Zepler Institute for Photonics and Nanoelectronics, University of Southampton, Highfield, Southampton, SO17 1BJ, UK

ARTICLE INFO

Keywords:
Active optical material
Bismuth
Phosphosilicate
Aluminosilicate
Spectroscopy
Optical amplifier

ABSTRACT

Bismuth (Bi)-doped aluminosilicate, phosphosilicate, germanosilicate and high (≥50 mol%) germanosilicate fibers have shown luminescence around 1.15 μm, 1.3 μm, 1.45 μm and 1.7 μm, respectively. Bi-doped fibers have paved the way for developing optical amplifiers and fiber lasers in the wavelength region of 1150–1500 nm and 1600–1700 nm, where it can serve a wide range of applications in astronomy, imaging, medicine and advanced optical communications. However, spectroscopic study is required to understand the nature of near-infrared (NIR)-emitting Bi active centers (BACs) to improve the efficiency of Bi-doped fiber amplifiers and lasers. In this paper, we review the luminescence properties of Bi-doped glasses as well as Bi-doped fibers with aluminosilicate, phosphosilicate, and germanosilicate glass hosts. Absorption and emission cross-sections of Bi-doped phosphosilicate fibers are reported. In addition, we review the current state of the art of Bi-doped fiber amplifiers development in the second telecom window (O-band) and in the E-band and S-band for the next-generation high-capacity optical communications.

1. Introduction

Since the appearance of the first erbium (Er)-doped fiber amplifier in 1987 as a breakthrough technology, rare earth (RE)-doped fibers have been well developed and widely used in the NIR region over the years, for many important applications including medicine, optical communications, and material processing, etc. Ytterbium (Yb), Er, thulium (Tm) and holmium (Ho)-doped fibers in silica glass host are operating in the wavelength bands around 1 μm, 1.5 μm, 1.8 μm and 2 μm, respectively. It has been a compelling research area to explore and establish new active materials as the gain media in optical fibers to develop amplifiers and lasers, in the missing wavelength bands of 1150–1500 nm and 1600–1700 nm which are not covered by RE elements. Bi-doped silica-based fibers stood out as reported to demonstrate an ultra-broadband NIR emission within different glass hosts spanning the O-, E−, S- and U-bands, as presented in Fig. 1 [1–3]. Bi-doped aluminosilicate fibers (BASFs) and Bi-doped phosphosilicate fibers (BPSFs) have showed luminescence in the wavelength bands of 1.1–1.2 μm and 1.3–1.4 μm, respectively. Bi-doped silicate fibers (BSFs) and Bi-doped germanosilicate fibers (BGSFs) can produce luminescence around 1.45 μm. Moreover, with a high content (≥50 mol%) of germanium dioxide (GeO_2) in Bi-doped germanosilicate fibers (BHiGSFs), the luminescence spectrum can be extended to 1.7 μm. Much exciting progress has been made in Bi-doped fiber amplifiers development, in the O-band, O + E-band and E + S-band using Bi-doped fibers co-doped with phosphorus (P) or germanium (Ge), as well as in the wavebands from 1100 to 1250 nm and from 1600 to 1800 nm using Bi-doped fibers co-doped with aluminium (Al) and with high content of Ge, respectively.

However, to achieve the efficient and robust amplification that supports a broad wavelength range has been a challenge. Associated spectroscopic characterization is required to help steer Bi-doped fiber development. Two main concerns should be addressed for designing and improving the performance of Bi-doped fiber amplifiers. Firstly, the Bi states that determine NIR emission are currently not fully understood. It is critical to identify the desired valence state, which depends on preform fabrication and fiber drawing conditions. Secondly, an increasing Bi concentration can result in increases in background loss (BL) and unsaturable loss (UL). The current generation of Bi-doped fibers that can be used in optical fiber amplifiers are mostly with a low Bi concentration of ≤0.1 mol%, which leads to the demand for long (100's meter) device lengths.

Bi has the electronic configuration of (Xe) $4f^{14}\ 5\ d^{10}\ 6s^2\ 6p^3$ which is different in comparison to commonly used RE elements. The inner subshells of Bi are completely filled and electrons from the outer layers 6s and 6p can have significant interactions with the host glass compositions. Therefore, Bi shows host dependent absorption and emission

* Corresponding author.
** Corresponding author.
E-mail addresses: Yu.Wang@soton.ac.uk (Y. Wang), jks@orc.soton.ac.uk (J. Sahu).

https://doi.org/10.1016/j.omx.2022.100219
Received 10 October 2022; Received in revised form 20 November 2022; Accepted 30 November 2022
Available online 22 December 2022

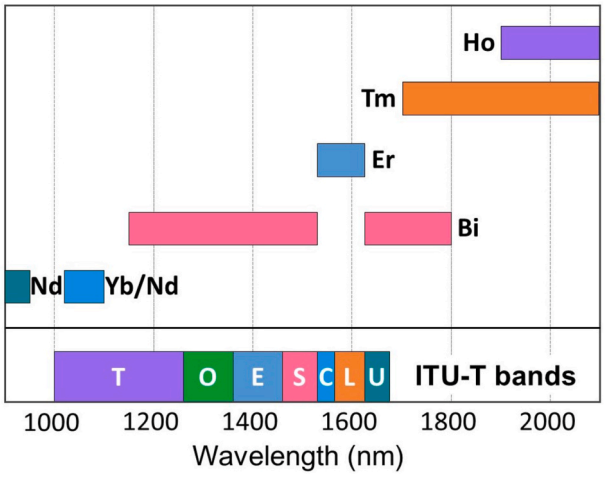

Fig. 1. Spectral regions covered by Bi and RE elements in silica glass host.

characteristics. Bi is a polyvalent element that exists with multiple oxidation states, i.e. Bi^{+}, Bi^{2+}, Bi^{3+}, and Bi^{5+}. It is important to generate the desired oxidation state in a controllable way in the optical preform and fibre fabrication. The balance of oxidation and reduction reactions during Bi-doped fiber fabrication procedures heavily depends on the fabrication conditions, such as atmosphere, temperature, glass compositions and concentration of each polyvalent element, which makes it difficult to manage Bi to the necessary oxidation states. There are a number of existing hypotheses on NIR-emitting Bi active centers (BACs), including Bi clusters [4], Bi^{+} [5,6], BiO [7], Bi ion dimers, e.g. Bi_2^-/Bi_2 or Bi_2^-/Bi_2^{2-} [8–10], Bi^{2+}-Bi^{3+} dimer or Bi^{+} between two vacancies [11], Bi^0 [12], $Bi^{5+}O_n^{2-}$ molecules [13–15], point defects [16], and Bi^{2+} + an oxygen vacancy [11,17]. Regardless of various theoretical and experimental assumptions, the origin of Bi related NIR-emitting centers is still under debates. Additional fundamental researches on the nature of NIR luminescence in Bi-doped fibers are required for improvement on the efficiency of Bi-doped fibre-based devices and systems.

In this paper, we review the luminescence properties of Bi-doped glasses and fibers, and report the recent progress on the absorption and emission cross-sections of Bi-doped optical fibers. Since the previous review on Bi-doped fibre amplifiers [2,18], many astonishing results have been achieved over the past one decade. We update the recent progress in Bi-doped fiber amplifiers, and review the state of the art of Bi-doped fiber amplifiers operating in different wavelength bands in the NIR region.

2. Bi-doped fibers

Since the first demonstration of NIR emission in a Bi-doped silica bulk glass [19] and the first fabrication of Bi-doped silicate optical fibers [43], various types of Bi-doped glasses and fibers have been established and reported with NIR luminescence. Table 1 summarizes compositions of diverse Bi-doped glasses and their luminescence properties, including silicate, germanate, borate, and phosphate glass systems. Besides, a few of Bi-doped chalcogenide and fluoride glasses are also demonstrated with NIR luminescence [44–47]. There are several important observations from Table 1:

- Bi-doped silica-based glasses with various co-dopants are the common types to produce broadband luminescence in the NIR region.
- The effective excitation bands are mostly located in the spectral range of 800–1600 nm where commercial laser diodes are available for pumping in the laser or amplifier systems.
- The luminescence spectra can contain more than one emission band. The luminescence bands are ultra-broad, of which the 3-dB bandwidth is usually in the range of 200–500 nm.
- The luminescence bandwidth and the locations of the luminescence bands are both dependent on the excitation wavelength and the glass compositions.

These exceptional features of Bi-doped glasses suggest a great potential for developing ultra-broadband optical amplifiers within the spectral region of 1150–1500 nm and 1600–1700 nm. In addition to Bi-doped bulk glasses, S. V. Firstov et al. [48,49] measured the luminescence properties of Bi-doped optical fibers based on excitation and emission wavelengths in the spectral region from 450 to 1700 nm. 4 types of Bi-doped fibers are studied: Bi-doped silicate ($Bi:SiO_2$) fibers (BSFs), Bi-doped germanate ($Bi:GeO_2$) fibers (BGFs), Bi-doped phosphosilicate ($Bi:P_2O_5$–SiO_2) fibers (BPSFs), and Bi-doped aluminosilicate ($Bi:Al_2O_3$–SiO_2) fibers (BASFs). The excitation and emission bands are reported in Refs. [2,49]. Work in Refs. [22,49] also predicted energy level diagrams of BACs associated with Si, Ge and P, determined from absorption and luminescence properties of BSF, BGF and BPSF samples, respectively. The main luminescence bands (as presented with the curves) and corresponding pump wavelength bands (as indicated with the arrows) that are commonly used in Bi-doped fibre amplifiers are summarized in Fig. 2 [50–56]. It is noteworthy that the luminescence of Bi-doped fibers within different silica-based glass hosts can cover the spectral region from 1100 nm to 1700 nm.

2.1. Bi-doped aluminosilicate, phosphosilicate and germanosilicate fibers

Various Bi-doped preforms and optical fibers are fabricated using MCVD in combination with vapor phase or solution doping technique [57]. A silica substrate tube serves as the fiber cladding. Bi and other co-dopants are incorporated into the fiber core from solution or through a vapor phase.

Fig. 3 presents the absorption spectrum of Bi-doped aluminosilicate fiber (BASF), phosphosilicate fiber (BPSF) and germanosilicate fiber (BGSF) with low GeO_2 content (~5 mol%), respectively. As can be seen, BASFs have effective absorption at wavelength bands 510 nm, 700 nm and from 900 to 1100 nm. BPSFs have effective absorption at wavelength bands 440 nm, 750 nm and from 1200 to 1300 nm. For BGSFs, the effective absorption is shown at wavelength bands 440 nm, 820 nm and from 1250 to 1400 nm. All three fiber samples show a broad absorption band in the NIR region. The fluorescence lifetime of BASFs is in the range of 820–860 μs at 1120 nm. For BPSFs, the fluorescence lifetime at 1267 nm is ranging from 740 to 780 μs. Unsaturable absorption of BASF, BPSF and BGSF samples are measured at their pump wavelengths and summarized in Fig. 4. In a UL measurement, the fibre absorption is measured as a function of the pump power that is launched into the fibre. A typical unsaturable loss measurement is shown in the inset of Fig. 4 for a BPSF sample. The small signal absorption and the unsaturable absorption of a BPSF sample are found to be 0.58 dB/m and 0.09 dB/m, respectively, which gives the UL of the BPSF sample as 15.5%. For BASF, two samples are measured at two pump wavelengths of 1047 nm and 1120 nm. For BPSF, different fiber samples are measured at a pump wavelength of 1240 nm. For BGSF, one sample is measured at three pump wavelengths of 1270 nm, 1310 nm and 1432 nm, respectively. It can be noticed that, the UL of BASFs is strongly pump wavelength dependent, whereas there is no significant difference in UL at different pump wavelengths for BGSFs. Also, it can be observed that the UL of BPSFs can vary significantly with fabrication conditions, which are very critical for controlling the UL in Bi-doped fibers. Moreover, what is noteworthy is that the UL of BPSFs can already be controlled within the 10–20% range. However, BASFs show a relatively high UL at above 30%. We will in due course improve the fabrication processes to reduce the UL of Bi-doped fibers moving forward.

Fig. 5, Fig. 6, Fig. 7 present the fluorescence spectra of BASF, BPSF and BGSF samples excited at their pump wavelengths, respectively. For BASFs, emission peaks are located at 1120 nm and 1160 nm, with the full width at half maximum (FWHM) of 140 nm and 135 nm,

Table 1
Luminescence properties of Bi-doped glasses.

Category	Compositions, mol%	λ_p, nm	λ_{em}, nm	FWHM, nm	Ref
Silicate	Bi:SiO_2	710	1150	150	[19]
	97.5SiO_2-2.2Al_2O_3-0.3Bi_2O_3	500	1140	200	[20]
	SiO_2:Bi	375/450	585,830,1440		[21]
	100SiO_2:Bi	240/375/422	827,1417		[22]
	5GeO_2-95SiO_2:Bi	365	1665		
		455	1646		
	3Al_2O_3–97SiO_2:Bi	510	1100		
		250	1250		
	10P_2O_5–90SiO_2:Bi	353	1300		
		427	1277		
	65SiO_2–30SrO–5Al_2O_3–2Bi_2O_3	808	1315	200	[23]
	65SiO_2–30BaO–5Al_2O_3–2Bi_2O_3	808	1325	200	[24]
	65SiO_2–30CaO–5Al_2O_3–2Bi_2O_3	808	1305	205	[25]
	50SiO_2–30GeO_2–15MgO–5Al_2O_3–1Bi_2O_3	808	1280	355	[26]
		980	1155	250	
	72SiO_2–2Al_2O_3–13Na_2O–8CaO- –4MgO–1K_2O–0.5Bi_2O_3–1.5C	800	1070,1300		[27]
	55.6SiO_2–22.2Al_2O_3–22.2MgO–1Bi_2O_3	700	1100–1300		[28]
		800	1200–1600		
	50SiO_2–25Al_2O_3–25CaO–0.5Bi_2O_3	690	1100	160	[29]
		909	1300	220	
	37.5SiO_2–25Al_2O_3–12.5P_2O_5–25CaO–0.5Bi_2O_3	690	1100	180	[29]
		909	1300	260	
	95.2SiO_2–2.63Al_2O_3–2.13GeO_2–0.04Bi_2O_3, in [wt%]	808	1240	300	[30]
		940/980	1130	170	
	43SiO_2–23Al_2O_3–20GeO_2–13Li_2O–1Bi_2O_3	808	1260	300	[31]
		808	1245	300	[32]
	40SiO_2–40CaO–20MgO–4Bi_2O_3	940	1235,1426		
		980	1235		
	95.5SiO_2–4.5Al_2O_3–0.01Bi_2O_3	480/695	1120	155	[33]
Germanate	75GeO_2–20SrO–5Al_2O_3–1Bi_2O_3	808	1279	225	[34]
		980	1231	510	
	96.5GeO_2–1.5Ga_2O_3–1.5Al_2O_3–0.5Bi_2O_3	808	1110		[35]
		980	1240		
	75GeO_2–20MgO–5Al_2O_3–0.5Bi_2O_3	880	1090,1290		[36]
	75GeO_2–20MgO–5Al_2O_3–1Bi_2O_3	880	1100,1300		
	75GeO_2–20MgO–5Al_2O_3–2Bi_2O_3	880	1300		
	75GeO_2–20MgO–5Al_2O_3–4Bi_2O_3	880	1325		
	75GeO_2–20MgO–5Al_2O_3–6Bi_2O_3	880	1375		
	89GeO_2–10Ta_2O_5–1Bi_2O_3	808	1250	250	[37]
Borate	75B_2O_3–20BaO–5Al_2O_3–2Bi_2O_3	808	1252	230	[6]
	65B_2O_3–30BaO–5Al_2O_3–2Bi_2O_3	808	1272	230	
	55B_2O_3–40BaO–5Al_2O_3–2Bi_2O_3	808	1300	194	
	5 mol%Bi:SrB_4O_7	808	1291	202	[38]
	75B_2O_3–25Bi_2O_3	808	1200		[39]
	75B_2O_3–15BaO–5Al_2O_3–1Bi_2O_3	800	1250		[40]
Phosphate	Bi:Li_2O–La_2O_3–Al_2O_3–B_2O_3–P_2O_5	800	1150		[41]
		980	1280		
	75P_2O_5–15B_2O_5–9Al_2O_3–1Bi_2O_3	808	1260	253	[42]
		980	1148	269	
	82P_2O_5–17Al_2O_3–1Bi_2O_3	808	1300	300	[5]
		980	1194		

respectively, when excited at wavelengths of 1047 nm and 1120 nm. BPSFs show emission peaks at 1280 nm, 1310 nm and 1340 nm, with the FWHM of 145 nm, 143 nm and 150 nm, while pumped at 1200 nm, 1267 nm and 1310 nm, respectively. For BGSFs excited at wavelengths of 1270 nm, 1304 nm and 1340 nm, no significant variation is observed in the emission peak locations that appear at 1403 nm, 1410 nm and 1420 nm, respectively. The emission peak bandwidth is relatively narrower with a FWHM of 133 nm, 114 nm and 107 nm correspondingly.

2.2. Absorption and emission cross-sections of Bi-doped phosphosilicate fibers

There are only very few existing work that reports on the absorption and emission cross-sections of BPSFs [58,59]. In this section, we characterize and present the absorption and emission cross-section spectra for the in-house fabricated BPSFs using saturation fluorescence method and Füchtbauer-Ladenburg (FL) equation, respectively.

Fig. 8 represents the refractive index profile for BPSF-1 as well as Bi_2O_3 and P_2O_5 distribution measured by Electron Probe Micro Analysis (EPMA). The refractive index of BPSF-1 shows an M-shape radially, with a maximum index difference Δn of around 0.004 between the core and the cladding, from which the P_2O_5 content is estimated as ~4 mol%. The Bi concentration is relatively low - at the level of 0.01 mol%. Saturation fluorescence method provides the determination of the absorption cross-section (σ_a) in active fibers [60,61]. It is based on that the fluorescent power is proportional to the population inversion n_2 on the upper energy level 2. For an infinitesimal segment of fiber, n_2 can be given by

$$n_2 = \frac{W_{12} N_{BAC}}{W_{12} + \frac{1}{\tau_{fl}}} \tag{1}$$

where, τ_{fl} is the fluorescence lifetime, N_{BAC} is the concentration of BACs in the fiber, W_{12} is the pump rate from the lower level 1 to the upper level 2. To reach half of the maximum fluorescence, i.e., to get a population inversion of $\frac{N_{BAC}}{2}$, the pump rate W_{ij} should be equal to $\frac{1}{\tau_{fl}}$. The stimulated rate between the lower level *i* and the upper level *j* is given by

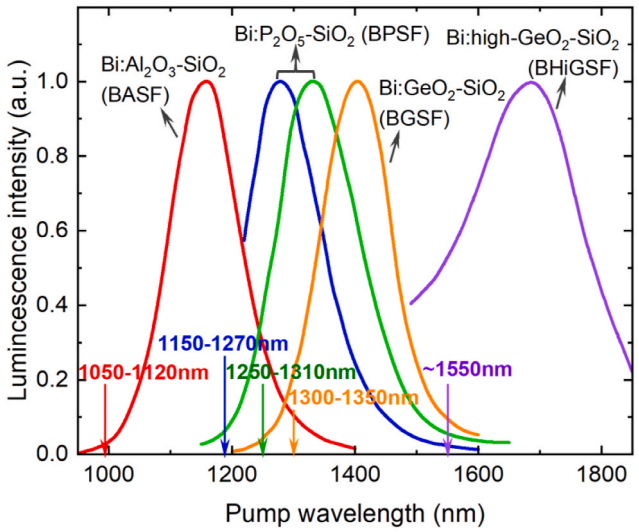

Fig. 2. Main pump wavelengths and luminescence bands of major Bi-doped silica-based fibers within different glass hosts that are commonly used in Bi-doped fiber amplifiers.

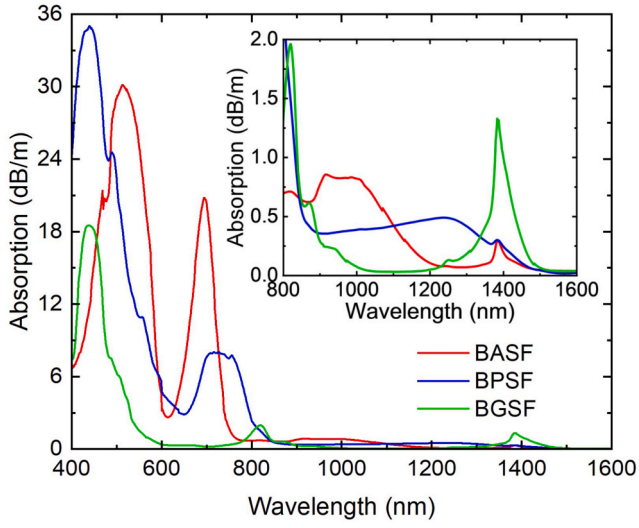

Fig. 3. Absorption spectrum of BASF, BPSF and BGSF samples. The inset shows the detailed absorption from 800 nm to 1600 nm.

$$W_{ij} = \frac{\sigma_{ij} P_p}{h\nu_{ij} A} \tag{2}$$

where, σ_{ij} is the absorption cross-section of this transition, P_p is the pump power, $h\nu_{ij}$ is the photon energy, and A is the effective mode field area. Derived from equations (1) and (2), the saturation fluorescence power P_{sat}, which is the pump power required to reach half inversion, can be written as

$$P_{sat} = \frac{h\nu_{12} A}{\sigma_{12}\tau_{fl}} \tag{3}$$

In saturation fluorescence measurements, the fluorescent power is measured as a function of pump power. The fluorescent power increases asymptotically with the increasing pump power to an upper limit corresponding to a full population inversion. The saturation fluorescence power and thereby the absorption cross-section at the pump wavelength can be calculated using equation (3).

The fluorescence spectrum of a BPSF sample is measured with an increasing pump power. The fluorescent power is obtained by integrating the fluorescence in the wavelength range from 1100 to 1600 nm and presented as a function of pump power (Fig. 9). Note that a short fiber length of less than 0.5 m is used here to avoid any influence from fluorescence re-absorption or ASE accumulation. The saturation fluorescence power P_{sat}, i.e. the pump power required to realize half of the maximum fluorescence, can be then obtained accordingly.

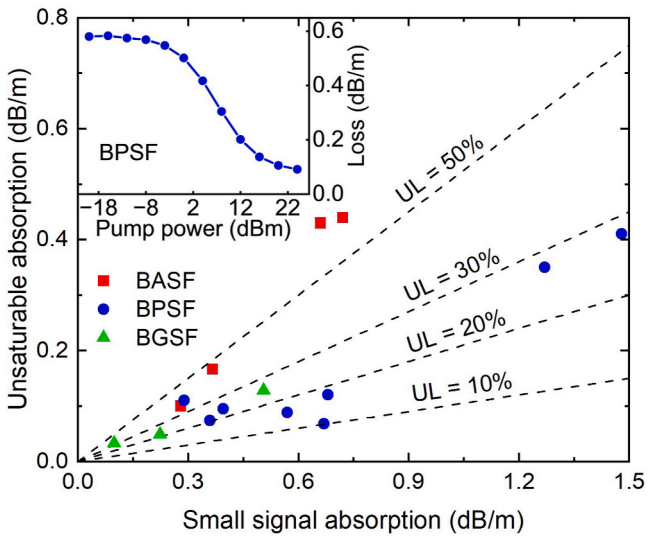

Fig. 4. Unsaturable loss of BASF, BPSF and BGSF samples measured at their pump wavelengths (BASF - 1047 nm, 1120 nm; BPSF - 1240 nm; BGSF - 1270 nm, 1310 nm, 1432 nm). The inset shows a typical UL measurement of a BPSF sample.

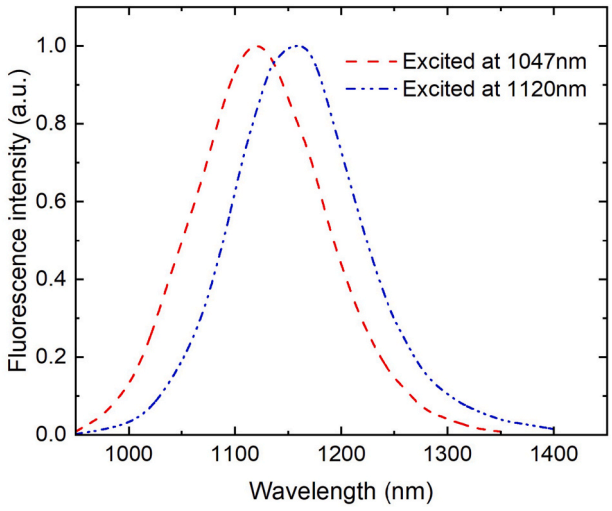

Fig. 5. Fluorescence spectra of BASF sample.

The saturation fluorescence measurements are accomplished for three different BPSFs-1, 2 and 3 at pump wavelengths of 1200 nm, 1267 nm and 1310 nm, respectively. Using the measured saturation fluorescence power P_{sat}, the absorption cross-sections at the corresponding pump wavelengths can be then analyzed using equation (3). Fig. 10 shows the absorption cross-sections measured via saturation fluorescence method at wavelengths of 1200 nm, 1267 nm and 1310 nm (as presented with the scatter data) and the predicted absorption cross-section spectrum using Gaussian curve fitting (as indicated with the dashed lines) for three different BPSFs. The results for BPSF-1, 2 and 3 are highly consistent - the absorption cross-section spectrum shows a maximum absorption cross-section of ~2.7 p.m.^{2} located at around 1295 nm with a FWHM of ~200 nm.

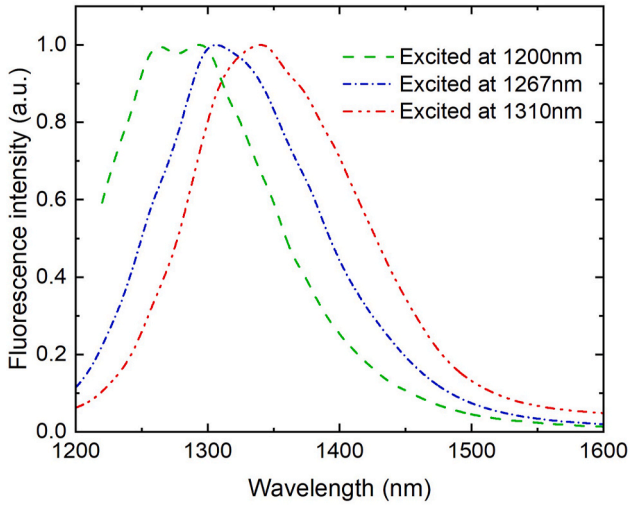

Fig. 6. Fluorescence spectra of BPSF sample.

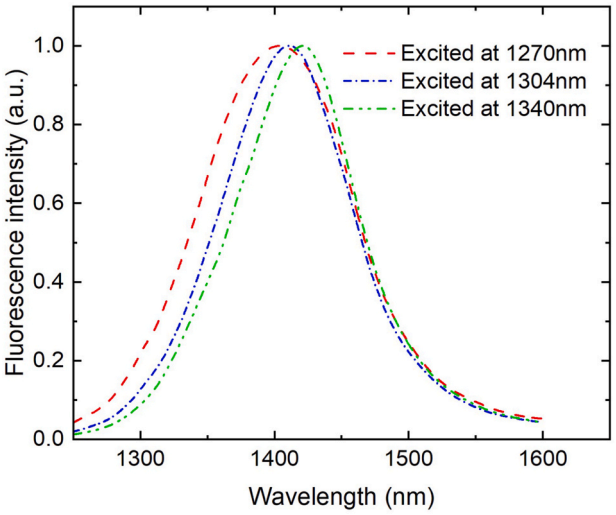

Fig. 7. Fluorescence spectra of BGSF sample.

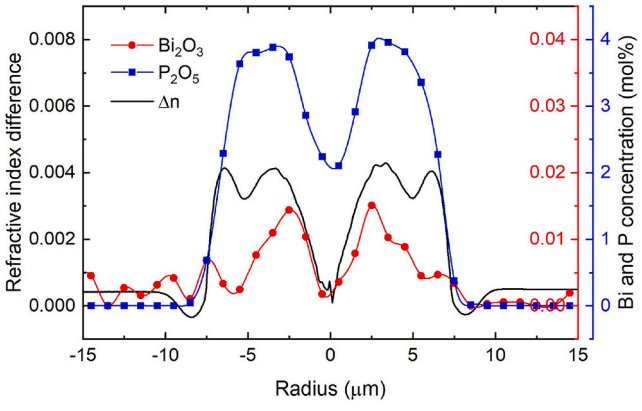

Fig. 8. Refractive index profile and Bi_2O_3 and P_2O_5 distribution of BPSF-1.

On the other hand, the emission cross-section (σ_e) of BPSFs can be directly calculated from the measured fluorescence spectrum using FL equation. The FL equation is derived from the Einstein relations with A and B coefficients. The Judd-Ofelt theory relates the cross-sections to the

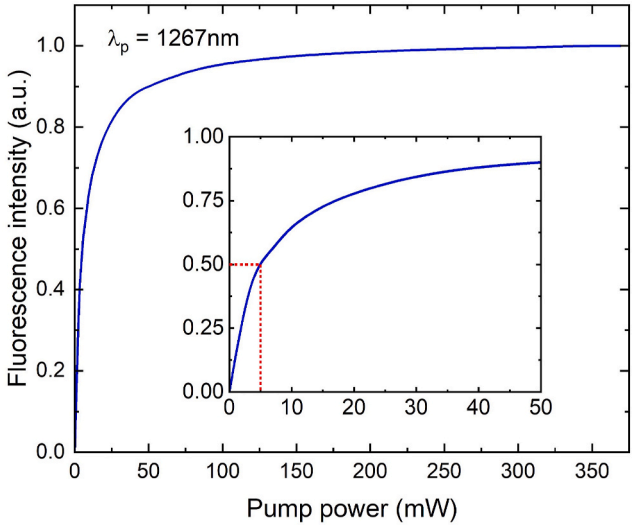

Fig. 9. Saturation fluorescence measurement of BPSF sample. The inset shows the obtained saturation pump power P_{sat}.

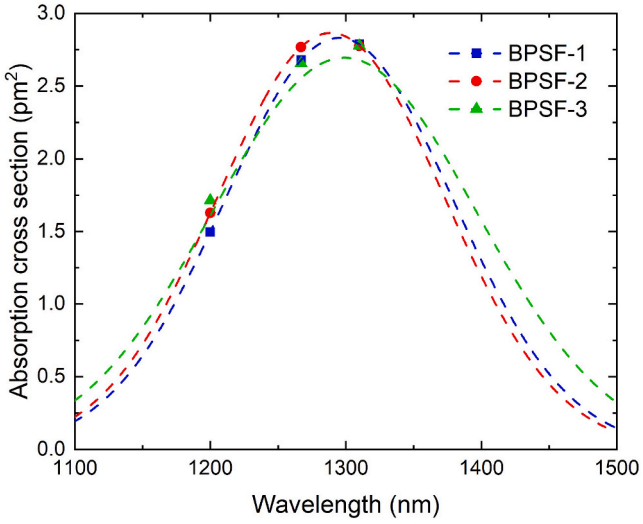

Fig. 10. Absorption cross-sections measured by saturation fluorescence method for BPSF-1, 2 and 3 at pump wavelengths of 1200 nm, 1267 nm and 1310 nm. The scatter represents the measured absorption cross-section data by the saturation fluorescence method. The dashed lines are the absorption cross-section spectrum predicted using Gaussian curve fitting.

transition probability $A_{21} = \frac{1}{\tau_{fl}}$ (τ_{fl} is the observed fluorescence lifetime), leading to the FL relation as follows [62]:

$$\sigma_e(\lambda) = \frac{\lambda^4}{8\pi n^2 c} \frac{I(\lambda)}{\tau_{fl} \Delta\lambda_{eff}} \tag{4}$$

where, λ is the signal wavelength, n is the medium refractive index, c is the vacuum velocity of light, $I(\lambda)$ is the normalized fluorescence spectrum, and $\Delta\lambda_{eff}$ is an effective line width defined by $\Delta\lambda_{eff} = \int I(\lambda) d\lambda$. The mean wavelength ($\bar{\lambda}$) of the transition can be used instead of λ in case of a narrow emission bandwidth. Using the line shape function $g(\lambda) = \frac{I(\lambda)}{\int I(\lambda) d\lambda}$, the FL equation can be expressed as:

$$\sigma_e(\lambda) = \frac{(\bar{\lambda})^4}{8\pi n^2 c \tau_{fl}} \frac{I(\lambda)}{\int I(\lambda) d\lambda} \tag{5}$$

The equation can be modified more accurate for cases with broader

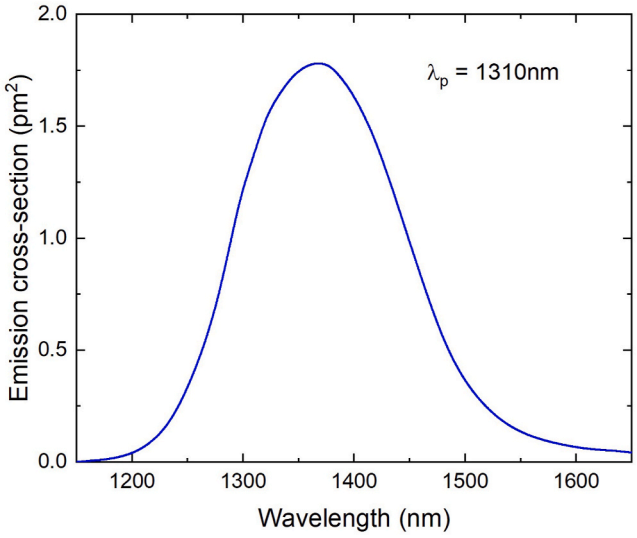

Fig. 11. Emission cross-section spectrum calculated by FL equation for BPSF sample.

Table 2
Absorption (σ_a) and emission (σ_e) cross-sections of Bi-doped phosphosilicate fibers as previously reported in the literature and in this work.

	Peak value, pm^2	Peak wavelength, nm	Method	Ref
σ_a	2.5±0.4	1240	Average BACs-P concentration	[58]
	2.1±0.3	1240	(1) Average BACs-P concentration (2) Measured g/α ratio	[59]
	~2.7	1295	Saturation fluorescence method	This work
σ_e	1.7	1325	Füchtbauer-Ladenburg equation	[58]
	1.6	1330	McCumber theory	[59]
	1.8	1360	Füchtbauer-Ladenburg equation	This work

emission bandwidth, e.g. Bi-doped fibers, by introducing a factor of $\left(\frac{\lambda}{\lambda}\right)^5$ [63]:

$$\sigma_e(\lambda) = \frac{\lambda^5}{8\pi n^2 c \tau_{fl}} \frac{I(\lambda)}{\int \lambda I(\lambda) d\lambda} \quad (6)$$

The fluorescence spectrum for BPSF sample is measured at a pump wavelength of 1310 nm, and the emission cross-section spectrum is determined from the fluorescence spectrum by FL equation in (6) (Fig. 11). The emission cross-section spectrum shows a maximum emission cross-section of ~1.8 $p.m.^2$ located at around 1360 nm. Table 2 compares the absorption and emission cross-sections of BPSFs as previously reported in the literature and in this work.

3. Bi-doped fiber amplifiers

3.1. Bi-doped fiber amplifiers in the O-band (1260–1360 nm) for optical communications

There has been great interest in developing optical fiber amplifiers in the O-band (1260–1360 nm) to operate with a comparable performance to EDFAs. The interest stems from the fact that most of the existing transmission fibers installed in the global physical infrastructure have the zero dispersion near 1.3 μm. It provides an opportunity of a rapid adoption and a low-cost capacity increase in the current optical communication systems. In this section, we review the continuous

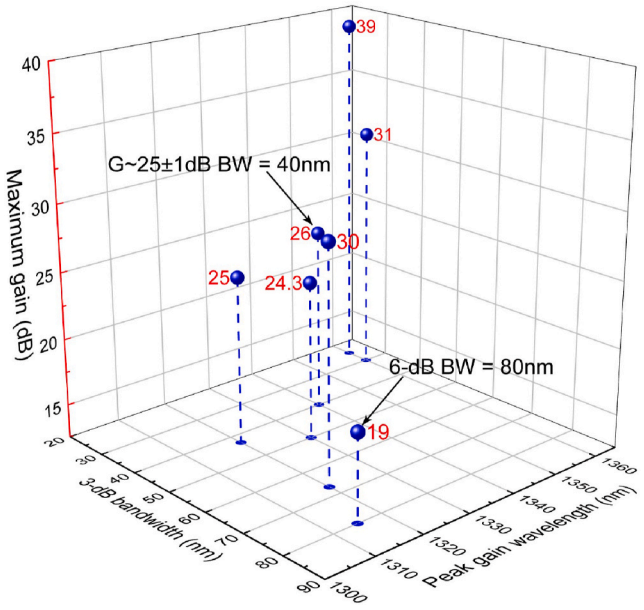

Fig. 12. Maximum gain and 3-dB bandwidth with the corresponding peak gain wavelength of Bi-doped fiber amplifiers operating in the O-band (1260–1360 nm) [51,64–69]

progress on the development of O-band BDFAs in recent years. A summary of the key results in O-band BDFA work is presented in Fig. 12, where the maximum gain value is marked in red for the work reported.

The first report of a positive net gain in the O-band is from a Bi-doped phosphogermanosilicate fiber (BPGSF). A pump power of 460 mW is used at a pump wavelength of 1230 nm, and the positive net gain covers from 1283 to 1372 nm [70]. Consequently, there has been consistent success of BDFA demonstrations in the O-band. In 2016, by using a combination of dual pump wavelengths at 1240 nm and 1267 nm, a flat gain of 25±1 dB and a NF of <6 dB is demonstrated with a 40 nm bandwidth from 1320 nm to 1360 nm using a 150 m long BPSF [64]. The BDFA is tested in both coarse and dense wavelength division multiplexing (WDM) experiments over a >100 km transmission link, providing a >22 dB gain over 50 nm (approximately 8.4 THz) in the O-band [71–73]. The double pass configuration is used in an O-band BDFA for the first time in 2011. It shows a 100% gain improvement from 1 dB to 2 dB compared with the same BDFA in a single pass configuration [74]. Further in 2019, O-band BDFAs using a double pass configuration are reported to provide high gains of 31 dB for a −10 dBm input signal [65] and 40 dB for a −23 dBm input signal [51] with a pump-to-signal power conversion efficiency of 11%. The temperature dependent gain performance of the O-band BDFAs are characterized in both the single pass and double pass configurations for a temperature range from −60 °C to +80 °C. The temperature-dependent-gain (TDG) coefficient of the O-band BDFAs is found to be in the range of −0.08 dB/°C to −0.02 dB/°C, which is similar to that of EDFAs and indicates a robust thermal stability [75,76]. At that point, the Bi-doped fibers used in BDFAs have a long length exceeding 100 m because of the low Bi concentration in fibers. In 2020, by pumping at 1.18 μm and gain clamping at 1.27 μm, an O-band BDFA is reported to provide a 30 dB peak gain with a 67 nm bandwidth from 1287 nm to 1354 nm, using a BPSF of only 36 m [66]. In the recent years, a novel W-type fiber structure is introduced in the Bi-doped fibers to improve the amplifier performance. In 2020, using a BPSF with a depressed cladding (DC), a compact BDFA is demonstrated in the O-band to provide a 20 dB gain for signals from −40 dBm to −10 dBm in the wavelength range of 1300–1350 nm [67,77]. A record gain coefficient of 0.18 dB/mW is reported at a pump wavelength of 1230 nm, with a pump-to-signal power conversion efficiency of >27%. Thanks to the bending-insensitive low-loss feature of the depressed

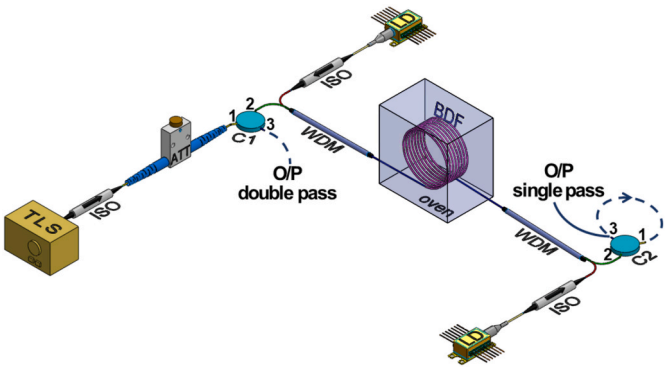

Fig. 13. Schematic of the O-band BPSF amplifier [52].

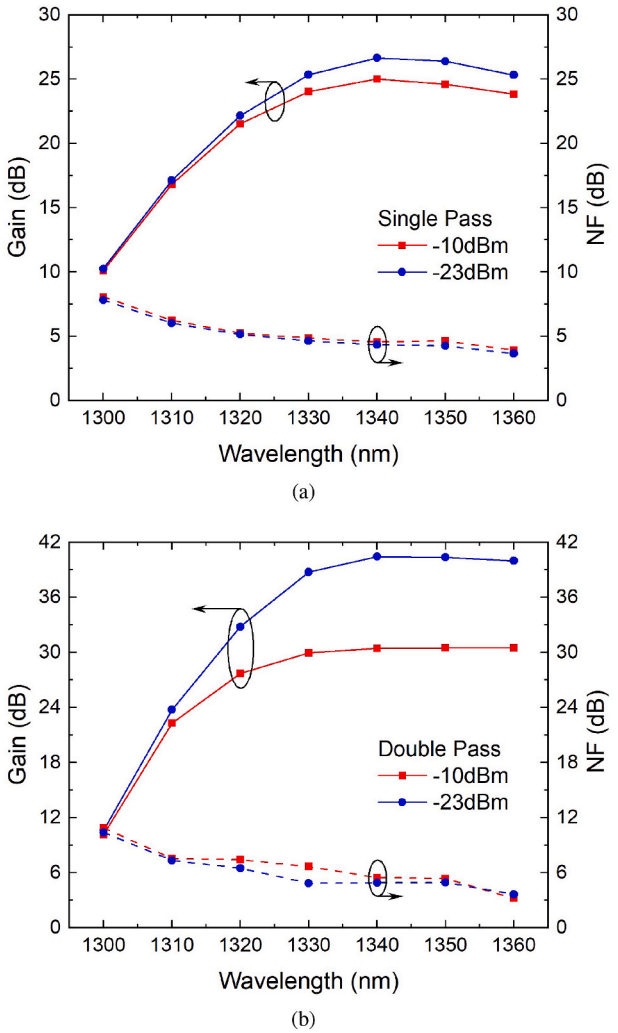

Fig. 14. Gain and NF spectrum of the O-band BDFA for signal powers of −10 dBm and −23 dBm in the (a) single pass and (b) double pass configurations.

cladding BPSF, the whole BDFA module is demonstrated with dimensions of 11.5 cm × 8 cm × 3.5 cm (L × W × H), with the 140 m long fiber coiled on a spool with a radius of 1.5 cm. In addition to the aforementioned demonstrations of the O-band BDFAs which are focused on the wavelength range from 1320 to 1360 nm, there are also BDFAs reported to be able to work at the short wavelength side of the O-band. In 2019, OFS laboratories demonstrate a BDFA capable of operating across the entire O-band using a 80 m long of BPSF [68,78]. It can

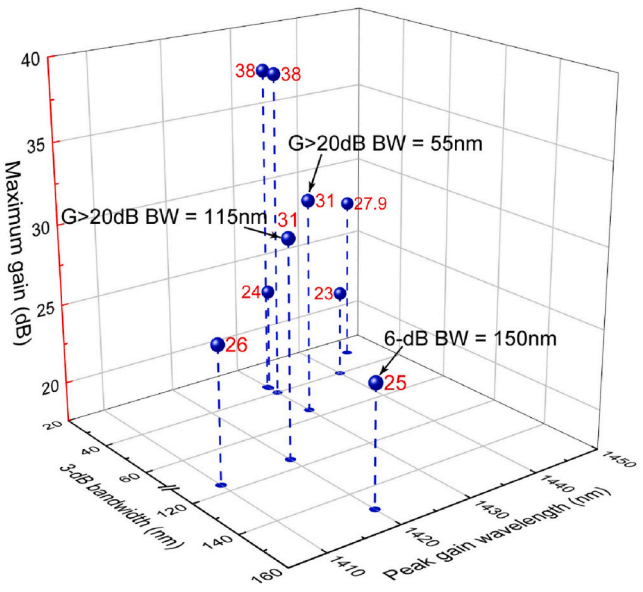

Fig. 15. Maximum gain and 3-dB bandwidth with the corresponding peak gain wavelength of Bi-doped fiber amplifiers operating in the wavelength band from 1300 to 1500 nm [54,55,80–86]

provide a 20 dBm output power with a 5 dB NF and a pump-to-signal power conversion efficiency of 20% over a 6-dB bandwidth of 80 nm. The gain peak can be flexibly centered from 1305 to 1325 nm by pump wavelength selection in the range from 1190 to 1240 nm. In 2021, an in-depth experimental characterization is accomplished on an O-band BDFA at University of Southampton, including electrical noise figure, gain tilt, transient response, and polarisation dependent gain. The findings confirms the suitability of the O-band BDFA for applications in high speed WDM systems [79].

3.11. 40 dB gain Bi-doped all-fiber amplifier operating in the O-band

Bi-doped phosphosilicate preforms were fabricated in-house using the MCVD-solution doping technique, with an index difference (Δn) of ~0.004 between the core and cladding. BPSFs were then drawn from the preforms with the core and cladding diameters of 15 μm and 125 μm. The absorption at a pump wavelength of 1270 nm is 0.47 dB/m, and the unsaturable loss at 1240 nm is 15.5%. The BPSF was pumped bi-directionally by two laser diodes operating at 1270 nm. The experimental set up is shown in Fig. 13. Two circulators were utilized to construct either a single pass or a double pass amplifier configuration.

The gain and NF of a 210 m long of the BPSF were measured from 1300 to 1360 nm for input signals of −10 dBm and −23 dBm in the single pass or double pass configurations, respectively. The single pass BDFA showed gains of 26±1 dB and the double pass BDFA performed gains of 40±1 dB from 1330 to 1360 nm for a −23 dBm input signal (Fig. 14). The BDFA is characterized with the temperature varying from +80 °C to −60 °C, and the TDG coefficient is found to be in the range of −0.08 dB/°C to −0.02 dB/°C, illustrating an outstanding thermal stability of the O-band BDFA [52].

3.2. Wideband Bi-doped fiber amplifiers in the O + E-band and E + S-band (1300–1500 nm)

The development of BDFAs in the spectral region of 1300–1500 nm is primarily driven by the great demand for optical fibre amplifiers for high-speed data transmission in the extended telecommunication window beyond C- and L-band. Being spectrally adjacent to the EDFA also makes it advantageous to develop efficient BDFAs due to the convenience of available components in the market. Moreover, it is not beneficial either economically or technically to use a number of separate

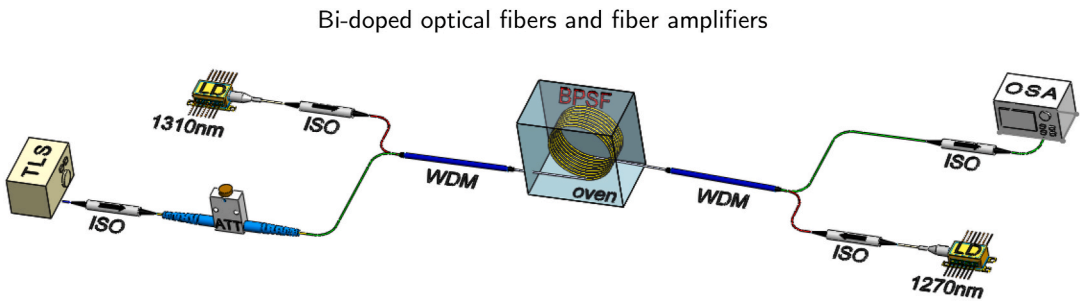

Fig. 16. Schematic of the O + E-band BPSF amplifier [54].

amplifiers in optical communications. Therefore, a single fiber amplifier with a broad gain bandwidth is preferred. In this section, we review the recent progress reported on the development of wideband BDFAs in the O + E-band and in the E + S-band. The key results of BDFA development in the wavelength band from 1300 to 1500 nm are summarized in Fig. 15, and the maximum gain values are marked in red.

An optical gain in the O- and E-band is firstly reported in 2008 from a single Bi-doped fiber, where a piece of BPGSF produced a positive on/off gain ranging from 1240 nm to 1485 nm with a dip near 1380 nm [87]. In 2011, an E-band BDFA is demonstrated providing a 24 dB peak gain at 1430 nm and a 3-dB bandwidth of ~40 nm, pumped at 1310 nm with a pump power of 65 mW [80,88]. There are many outstanding demonstrations of the O + E-band BDFAs ever since 2020. A BPSF is fabricated with a depressed cladding (DC) structure, of which the fiber loss in the spectral region from 1100 to 1400 nm is independent on the bending radius from 12 cm to 1.5 cm. Using the bend-insensitive Bi-doped fibers coiled at a radius of 1.5 cm, a compact BDFA is demonstrated with a positive gain from 1240 nm to 1460 nm [69]. In addition, by pumping at 1180 nm and gain clamping at 1280 nm, a wideband gain with a peak value of >25 dB and a 3-dB bandwidth of >135 nm is reported from a combination of a BPSF and a BGSF [81,89]. Furthermore, by using the bi-directional pumping at dual wavelengths of 1270 nm and 1310 nm, a wideband BDFA is demonstrated to provide >20 dB gain covering from 1345 nm to 1460 nm with a maximum gain of 31 dB at 1420 nm [53,90]. Using a double pass configuration, the BDFA gain is significantly improved in the E-band, providing a maximum gain of 38 dB at 1430 nm with a 3-dB bandwidth of 40 nm [55,90]. The temperature dependent gain performance of the O + E-band BDFA is characterized in both the single pass and double pass configurations, and the TDG coefficient is found to be in the range of −0.015 dB/°C to −0.002 dB/°C, illustrating an outstanding thermal stability of the O + E-band BDFAs [53,55,90]. Very recently, a record maximum gain of 38 dB operating from 1384 nm to 1484 nm is reported from a single-stage single-pass BDFA [86].

One major issue of the wideband BDFAs in the O- and E-band is the reduction in amplifier gain near 1380 nm, which is induced by the OH content in the fibers. Some efforts have been reported on the reduction of OH concentration by progressing fiber fabrication techniques, which is promising to eliminate the dip in the gain spectrum. In 2021, using a BPSF with extremely low OH, an O + E-band BDFA is demonstrated with a flattop gain of >23 dB from 1325 nm to 1441 nm [82,91,92].

On the other hand, an optical gain in the E− and S-band is firstly reported in 2010 from a BPGSF, which shows a positive net gain from 1410 nm to 1600 nm, with a pump power of 190 mW at 1318 nm [70]. In 2020 and 2021, using a BGSF of >300 m and pumps at the wavelength of ~1320 nm, E + S-band BDFAs are demonstrated to operate in the spectral region from 1405 nm to 1500 nm with a peak gain of ~30 dB [83,84]. In 2022, BGSFs are fabricated with a W-type profile and a graded-index profile, and the amplifier gain characteristics of the BGSFs with W-type and graded-index structures are compared. An E + S-band BDFA with a 20 dB peak gain and a 40 nm bandwidth is demonstrated using a 120 m long W-type BGSF and a pump power of only 45 mW, of which the gain efficiency is reported to be 0.52 dB/mW [85]. In addition, a hybrid amplifier based on Bi-doped fiber and Er-doped fiber is reported to produce a >27 dB gain and an output power of 24.5 dBm from 1431 nm to 1521 nm [93,94].

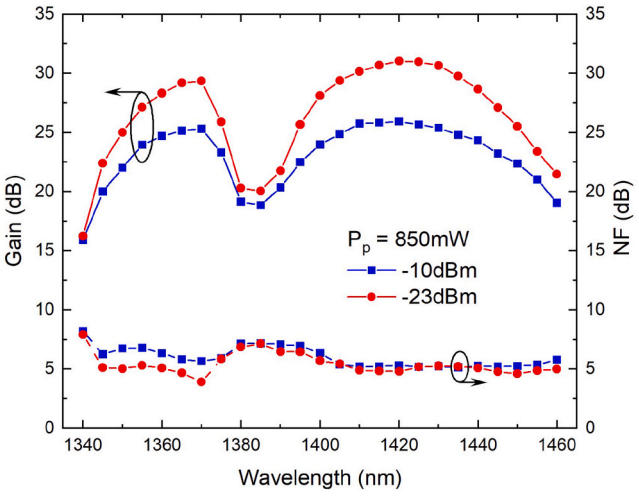

Fig. 17. Gain and NF spectrum of O + E-band BDFA for signal powers of −10 dBm and −23 dBm.

3.2.1. *Ultra-broadband Bi-doped fiber amplifier covering a 115 nm bandwidth in the O + E-band*

The in-house fabricated Bi-doped phosphosilicate preforms via MCVD-solution doping technique were drawn into fibers with the refractive index difference (Δn) of ~0.004 and the core and cladding diameters of 11 μm and 150 μm. The absorption at pump wavelengths of 1270 nm and 1310 nm is 0.57 dB/m and 0.52 dB/m, respectively. The unsaturable loss at 1240 nm and 1432 nm is 16.4% and 16.3%, respectively. The BPSF was pumped bi-directionally using two laser diodes at dual pump wavelengths of 1270 nm and 1310 nm. The experimental set up is shown in Fig. 16.

The gain and NF characteristics of the BPSF with a fibre length of 220 m is measured from 1345 to 1460 nm (Fig. 17). An ultra-broadband gain of >20 dB and a NF of 4.6 ~7.1 dB were achieved in the wavelength band from 1345 nm to 1460 nm. An overall gain of 22.5±3.5 dB and 25.5±5.5 dB was obtained over the 115-nm bandwidth for −10 dBm and −23 dBm input signals, respectively. The OH concentration in the BPSF is 1.2 ppm. The lowest gain of ~20 dB with a correspondingly higher NF of ~7 dB at around 1380 nm is caused by the OH absorption in the BPSF, and thereby the double hump gain spectrum is not intrinsic to the BPSFs and likely to be reduced or eliminated eventually by improving the drying process during fiber fabrications. The temperature dependent performance of the O + E-band BDFA is characterized from +80 °C to −60 °C, and The TDG coefficient is obtained in the range of −0.08 dB/°C to −0.01 dB/°C for different input signals across the wavelength band from 1350 nm to 1460 nm, emphasizing a remarkable thermal stability

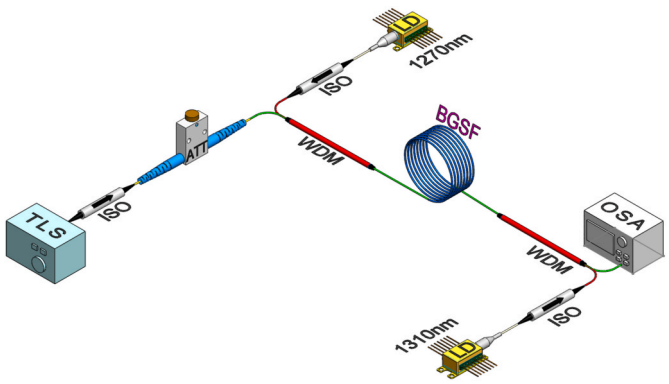

Fig. 18. Schematic of the E + S-band BGSF amplifier.

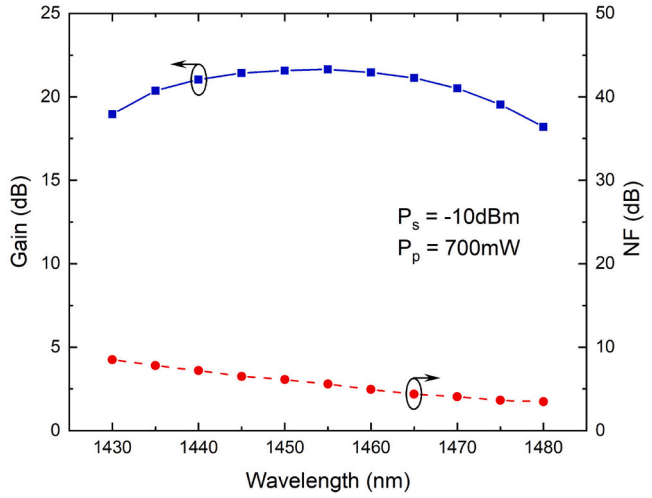

Fig. 19. Gain and NF spectrum of E + S-band BDFA for a signal power of −10 dBm.

of the ultra-broadband O + E-band BDFA [54].

3.2.2. Bi-doped fibre amplifier with a flat gain of 20 dB operating in the E + S-band

Bi-doped germanosilicate preform was fabricated using MCVD-solution doping technique with a refractive index difference (Δn) of ~0.01 between the core and cladding. BGSF was then drawn from the preforms with the core and cladding diameters of 7 μm and 100 μm. The BGSF was pumped bi-directionally using two laser diodes at pump wavelengths of 1270 nm and 1310 nm. The experimental set up is shown in Fig. 18. The pump wavelengths were optimized in order to provide the flat gain characteristics. The total available pump power that is launched into the BGSF is 250 mW from the 1270 nm laser diode and 450 mW from the 1310 nm laser diode. The absorption and the unsaturable loss of the BGSF are 0.2 dB/m and 22% at 1310 nm.

The gain and NF performance was measured using a 250 m long of the BGSF. A flat gain of 20±1.5 dB was achieved for a signal power of −10 dBm, with a 3-dB bandwidth of 50 nm from 1430 to 1480 nm operating in both the E− and S-band (Fig. 19). The temperature dependent performance of the E + S-band amplifier was tested within the temperature range from +80 °C to −60 °C. The gain and NF characteristics at different signal wavelengths from 1435 to 1480 nm all performed highly insensitive to the environmental temperature - the variation of gain and NF is within 1 dB across the 140°C temperature span, representing a robust thermal stability of the E + S-band BDFA. More details of the proposed E + S-band BDFA will be reported elsewhere.

3.3. Bi-doped fiber amplifiers in the wavebands from 1100 to 1250 nm and from 1600 to 1800 nm

Lasers and amplifiers in the wavelength range from 1100 to 1250 nm are required in many important applications, such as in astronomy for a laser guide star [96], in dermatology [97], in ophthalmology [98] and in optical sources with the development of visible light lasers through frequency doubling coming into sight. Recently, the wavebands near 1.1 μm has also drawn significant attention for applications in optical communications using low-loss hollow core fibers [99]. However, there are very limited progress on developing BDFAs in the 1.1 μm spectral region. In 2011, a maximum gain of 5 dB at 1180 nm is reported from a BASF using a watt-level pump power [100]. Later in 2015, an improved gain of 11.5 dB is demonstrated at 1180 nm using a 100 m long of BASF [50].

There are many medical applications of lasers and amplifiers in the wavebands from 1600 to 1800 nm, including laser surgery [101], endoscopy [102], optical coherence tomography [103] and biomedical imaging such as multi-phonon microscopy [104]. As this spectral region falls into the atmospheric transparency window, it is also used in remote optical sensing and detection [105]. In addition, the novel design of hollow core photonics crystal fibers with ultimate low loss near 1.8 μm enables the potential of optical communications in this waveband [106]. There are only a few study on the development of BDFAs near 1.7 μm to date. In 2016, a maximum gain of 23 dB at 1710 nm with a 3-dB bandwidth of 40 nm is reported using a 50 m long of BHiGSF pumped at 1550 nm with a pump power of 300 mW [56,107]. In 2020, a single-frequency BDFA is presented using a 90 m BHiGSF with output powers of 163 mW and 197 mW operating at 1651 nm and 1687 nm, respectively [108].

In addition to Bi-doped fiber amplifiers, there are superfluorescent sources demonstrated at 1.34 μm, 1.44 μm and 1.73 μm using BPSF and BGSF [109–111].

4. Conclusions

The field of Bi-doped fibers for optical amplifiers and fiber lasers has come into sight as an attractive research topic for the past one and a half decades. Much exciting progress has been made in Bi-doped fibers development with various co-dopants and the Bi-doped fiber amplifiers development in different wavebands. MCVD process in combination with vapor phase or solution doping, as the commercially adopted method for low-loss high-purity RE-doped fiber fabrication, is used to introduce Bi within diverse glass hosts including aluminosilicate, phosphosilicate, and germanosilicate. These Bi-doped fibers show the broadband absorption and emission characteristics in the NIR region, with a great potential as a novel gain medium in the wavelength bands of 1150–1500 nm and 1600–1700 nm. We emphasize that the absorption spectrum of BASF, BPSF and BGSF consists of multiple broad absorption bands, as well as the fluorescence spectrum is dependent on the pump wavelength which can cover a wide spectral range. For the first time, the saturation fluorescence method is adapted for the analysis of the absorption cross-sections of BPSFs.

Many successful demonstrations of efficient Bi-doped fiber amplifiers have been accomplished, especially in the O-band (the second telecommunication window), O + E− and E + S-band (from 1300 to 1500 nm). To date, maximum gains of 11.5 dB at 1.18 μm [50], 25 dB at 1.42 μm [81], and 23 dB at 1.7 μm [56] have been demonstrated using BASFs, a combination of BPSFs and BGSFs, and BHiGSFs, respectively. Moreover, maximum gains of 40 dB at 1.36 μm [51,52], and 38 dB at 1.43 μm [55] have been demonstrated using BPSFs. In particular, an efficient BDFA with a 40 dB gain is reported in the O-band [51], and an ultra-broadband BDFA operating in the O + E-band is demonstrated providing a >20 dB gain from 1345 to 1460 nm [53,54]. In addition, an E + S-band BDFA is demonstrated to offer a flat gain of 20±1.5 dB from 1430 to 1480 nm with a 3-dB bandwidth of 50 nm. Following the

Table 3
Summary of progress in Bi-doped fiber amplifiers.

Year	Ref	Fiber type	Length, m	Abs @λ_p, dB/m	UL @λ_p, %	λ_p/λ_s, nm	Gain/NF @λ_s, dB
2011	[80, 88]	BDF	125	0.47	8 [dB/km]	1310/1430	24,30/6
2015	[50]	BASF	100	0.7	35%	1047,1120/1180	11.5/N.A.
2016	[56]	BHiGSF	N.A.	0.92 [@1650 nm]	0.11 [dB/m]	1550/1710	23/7
2016	[64]	BPSF	150	1	7%	1240,1267/1350	26/5
2019	[65],[d]	BPSF	152	0.57	N.A.	1240,1270/1360	31/7
2019	[51],[d]	BPSF	152	0.57	15%	1270/1360	40/5
2019	[76],[d]	BPSF	212	0.5	13	1270/1350	39/4.2
2019	[52],[d]	BPSF	210	0.47	15.5%	1270/1350	40/4.8
2019 2020	[78, 68]	BPSF	80	N.A.	N.A.	1195-1235/ 1305–1325	19/5
2020	[95]	BPSF	31	3.06	N.A.	1240/1340	14.8/N.A.
2020	[77, 67]	DC-BPSF	140	0.45	13%	1230/1320	25/5-6
2020	[69]	DC-BPSF	108	~0.55	N.A.	1230/1322-1325	0.2 [dB/m]/N.A.
2020	[66]	BPSF	36	~0.6	N.A.	1180,1270/ 1287–1354	30/7
2020	[89],[b]	BPSF+ BGSF	93.5, 58	N.A.	N.A.	1180,1270/ 1306–1441	26/7.3
2020	[83]	BGSF	400	54 [dB]	N.A.	1350/1445	27.9/5
2020 2021	[53, 54],[b]	BPSF	220	0.57,0.52	16.4%	1270,1310/1420	31/4.8
2021	[84]	BGSF	320	N.A.	N.A.	1320/1430	31/4.75
2021	[91, 82],[b]	BPSF	150	0.41	8.3%	1256/1410	33/5.8
2021	[92],[b]	BPSF	150	0.42	6.7	1256/~1410	26/5-6
2021	[55],[d]	BPSF	220	0.57,0.52	16.4%	1270,1310/1430	38/6
2022	[85]	DC-BGSF	120	0.8 [@1410 nm]	N.A.	1330/1430	20/5.3
2022	[81],[b]	BPSF+ BGSF	93, 56	N.A.	N.A.	1180,1270/ 1300–1450	>25/7
2022	[86]	BGSF	400	N.A.	N.A.	1320/1430	38/4.5

[d] Using double pass configuration.
[b] Recognized as wideband amplifier.

impressive progress in optical amplifiers development using Bi-doped fibers, Table 3 summarizes reported Bi-doped fiber amplifiers, in terms of fiber type, pump and signal wavelength range, gain and noise figure (NF). Evidently, Bi-doped fibre amplifiers are rapidly growing towards not only high gain but also a broadband coverage. The temperature dependent characteristics of the aforementioned BDFAs are tested, ensuring the TDG coefficient is under −0.08 dB/°C [52,54].

With respect to the development of Bi-doped fibers for the amplifiers and lasers demonstrations, several concerns still remain in the way to be addressed. On one hand, the Bi concentration in the current generation of Bi-doped fibers is relatively low, which results in the requirements of a longer device length - 100's of meters. On the other hand, the increased amount of Bi in the core tends to induce additional fiber losses such as higher UL which is detrimental to optical amplifiers performance. Efforts should be focused on the fabrication of high concentration Bi-doped fibers with low loss, to develop Bi-doped fiber lasers and optical amplifiers with improved efficiency. As the most important challenge in doing so, significant attention should be paid to the origin of NIR luminescence in Bi-doped fibers. Resolving the nature of the Bi-related NIR-emitting active centers can certainly revolutionize the next generation of Bi-doped fiber lasers and optical amplifiers.

CRediT authorship contribution statement

Yu Wang: Conceptualization, of this study, Methodology, Data acquisition and, Formal analysis, Visualization, Writing – original draft. **Siyi Wang:** Preform fabrication. Preform and fiber characterization. **Arindam Halder:** Preform fabrication. **Jayanta Sahu:** Supervision, Project administration, Funding acquisition, Writing – review & editing.

Declaration of competing interest

The authors declare that they have no known competing financial interests or personal relationships that could have appeared to influence the work reported in this paper.

Data availability

Data will be made available on request.

Acknowledgements

The data for this work can be accessed at the University of Southampton Institutional Research Repository doi: https://doi.org/10.5258/SOTON/D2372. This work was supported by the Engineering and Physical Sciences Research Council (EPSRC) funded "AirGuide Photonics" Programme Grant and through a II-VI Foundation studentship (Y. Wang and S. Wang).

References

[1] S. Tanabe, Rare-earth-doped glasses for fiber amplifiers in broadband telecommunication, Compt. Rendus Chem. 5 (12) (2002) 815–824.
[2] E.M. Dianov, Bismuth-doped optical fibers: a challenging active medium for near-IR lasers and optical amplifiers, Light Sci. Appl. 1 (5) (2012) e12–e12.
[3] N. Thipparapu, Y. Wang, S. Wang, A. Umnikov, P. Barua, J. Sahu, Bi-doped fiber amplifiers and lasers, Opt. Mater. Express 9 (6) (2019) 2446–2465.
[4] M. Peng, J. Qiu, D. Chen, X. Meng, C. Zhu, Superbroadband 1310 nm emission from bismuth and tantalum codoped germanium oxide glasses, Opt. Lett. 30 (Sep 2005) 2433–2435.
[5] X. geng Meng, J. rong Qiu, M. ying Peng, D. ping Chen, Q. zhong Zhao, X. wei Jiang, C. shan Zhu, Near infrared broadband emission of bismuth-doped aluminophosphate glass, Opt Express 13 (Mar 2005) 1628–1634.
[6] X. geng Meng, J. rong Qiu, M. ying Peng, D. ping Chen, Q. zhong Zhao, X. wei Jiang, C. shan Zhu, Infrared broadband emission of bismuth-doped barium-aluminum-borate glasses, Opt Express 13 (Mar 2005) 1635–1642.
[7] J. Ren, Y. Qiao, C. Zhu, X. Jiang, J. Qiu, Optical amplification near 1300 nm in bismuth-doped strontium germanate glass, J. Opt. Soc. Am. B 24 (Oct 2007) 2597–2600.
[8] A. Bishay, S. Arafa, Gamma-induced absorption and structural studies of arsenic borate glasses, J. Am. Ceram. Soc. 49 (8) (1966) 423–430.
[9] S. Khonthon, S. Morimoto, Y. Arai, Y. Ohishi, Luminescence characteristics of Te- and Bi-doped glasses and glass-ceramics, J. Ceram. Soc. Jpn. 115 (1340) (2007) 259–263.
[10] V. Sokolov, V. Plotnichenko, E. Dianov, Origin of broadband near-infrared luminescence in bismuth-doped glasses, Opt. Lett. 33 (13) (2008) 1488–1490.
[11] E.M. Dianov, On the nature of near-IR emitting Bi centres in glass, Quant. Electron. 40 (4) (2010) 283.

[12] M. Peng, C. Zollfrank, L. Wondraczek, Origin of broad NIR photoluminescence in bismuthate glass and Bi-doped glasses at room temperature, J. Phys. Condens. Matter 21 (28) (2009), 285106.

[13] E. Kustov, L. Bulatov, V. Dvoyrin, V. Mashinsky, Molecular orbital model of optical centers in bismuth-doped glasses, Opt. Lett. 34 (10) (2009) 1549–1551.

[14] E. Kustov, L. Bulatov, V. Dvoyrin, V. Mashinsky, E. Dianov, Crystal field and molecular orbital theory of MB_m centres in glasses, J. Phys. B Atom. Mol. Opt. Phys. 43 (2) (2010), 025402.

[15] I. Razdobreev, V.Y. Ivanov, L. Bigot, M. Godlewski, E. Kustov, Optically detected magnetic resonance in bismuth-doped silica glass, Opt. Lett. 34 (17) (2009) 2691–2693.

[16] M.Y. Sharonov, A.B. Bykov, V. Petricevic, R.R. Alfano, Spectroscopic study of optical centers formed in Bi-, Pb-, Sb-, Sn-, Te-, and In-doped germanate glasses, Opt. Lett. 33 (Sep 2008) 2131–2133.

[17] E. Dianov, Nature of Bi-related near IR active centers in glasses: state of the art and first reliable results, Laser Phys. Lett. 12 (9) (2015), 095106.

[18] E.M. Dianov, Amplification in extended transmission bands using bismuth-doped optical fibers, J. Lightwave Technol. 31 (4) (2012) 681–688.

[19] K. Murata, Y. Fujimoto, T. Kanabe, H. Fujita, M. Nakatsuka, Bi-doped SiO_2 as a new laser material for an intense laser, Fusion Eng. Des. 44 (1–4) (1999) 437–439.

[20] Y.F.Y. Fujimoto, M.N.M. Nakatsuka, Infrared luminescence from bismuth-doped silica glass, Jpn. J. Appl. Phys. 40 (3B) (2001) L279.

[21] O.V. Laguta, H.E. Hamzaoui, M. Bouazaoui, V.B. Arion, I.M. Razdobreev, On the nature of photoluminescence in bismuth-doped silica glass, Sci. Rep. 7 (1) (2017) 1–6.

[22] E.G. Firstova, I. Bufetov, V.F. Khopin, V.V. Vel'miskin, S.V. Firstov, G. A. Bufetova, K.N. Nishchev, A.N. Gur'yanov, E.M. Dianov, Luminescence properties of IR-emitting bismuth centres in-based glasses in SiO_2-based glasses in the UV to near-IR spectral region, Quant. Electron. 45 (1) (2015) 59.

[23] J. Ren, L. Yang, J. Qiu, D. Chen, X. Jiang, C. Zhu, Effect of various alkaline-earth metal oxides on the broadband infrared luminescence from bismuth-doped silicate glasses, Solid State Commun. 140 (1) (2006) 38–41.

[24] J. Ren, J. Qiu, D. Chen, C. Wang, X. Jiang, C. Zhu, Infrared luminescence properties of bismuth-doped barium silicate glasses, J. Mater. Res. 22 (7) (2007) 1954–1958.

[25] J. Ren, J. Qiu, D. Chen, X. Hu, X. Jiang, C. Zhu, Luminescence properties of bismuth-doped lime silicate glasses, L5–L8, J. Alloys Compd. 463 (2008) 1–2.

[26] J. Ren, H. Dong, H. Zeng, X. Hu, C. Zhu, J. Qiu, Ultrabroadband infrared luminescence and optical amplification in bismuth-doped germanosilicate glass, IEEE Photon. Technol. Lett. 19 (18) (2007) 1395–1397.

[27] S. Khonthon, S. Murimoto, Y. Arai, Y. Ohishi, Near infrared luminescence from Bi-doped soda lime silicate glasses, Suranaree J. Sci. Technol 14 (2) (2007) 141–146.

[28] B. Denker, B. Galagan, V. Osiko, I. Shulman, S. Sverchkov, E. Dianov, Absorption and emission properties of Bi-doped Mg–Al–Si oxide glass system, Appl. Phys. B 95 (4) (2009) 801–805.

[29] Z. Song, Z. Yang, D. Zhou, Z. Yin, C. Li, R. Wang, J. Shang, K. Lou, Y. Xu, X. Yu, et al., The effect of P_2O_5 on the ultra broadband near-infrared luminescence from bismuth-doped SiO_2–Al_2O_3–CaO glass, J. Lumin. 131 (12) (2011) 2593–2596.

[30] L. Zhang, G. Dong, J. Wu, M. Peng, J. Qiu, Excitation wavelength-dependent near-infrared luminescence from Bi-doped silica glass, J. Alloys Compd. 531 (2012) 10–13.

[31] N. Zhang, J. Qiu, G. Dong, Z. Yang, Q. Zhang, M. Peng, Broadband tunable near-infrared emission of Bi-doped composite germanosilicate glasses, J. Mater. Chem. 22 (7) (2012) 3154–3159.

[32] P. Yu, L. Su, W. Guo, J. Xu, Broadband infrared luminescence in Bi-doped silicate glass, J. Non-Cryst. Solids 464 (2017) 34–38.

[33] A. Veber, M.R. Cicconi, A. Puri, D. de Ligny, Optical properties and bismuth redox in Bi-doped high-silica Al–Si glasses, J. Phys. Chem. C 122 (34) (2018) 19777–19792.

[34] J. Ren, J. Qiu, D. Chen, X. Hu, X. Jiang, C. Zhu, Ultrabroad infrared luminescence from Bi-doped aluminogermanate glasses, Solid State Commun. 141 (10) (2007) 559–562.

[35] S. Zhou, H. Dong, H. Zeng, J. Hao, J. Chen, J. Qiu, Infrared luminescence and amplification properties of Bi-doped GeO_2-Ga_2O_3-Al_2O_3 glasses, J. Appl. Phys. 103 (10) (2008), 103532.

[36] B. Xu, S. Zhou, D. Tan, Z. Hong, J. Hao, J. Qiu, Multifunctional tunable ultra-broadband visible and near-infrared luminescence from bismuth-doped germanate glasses, J. Appl. Phys. 113 (8) (2013), 083503.

[37] L. Wang, Y. Zhao, S. Xu, M. Peng, Thermal degradation of ultrabroad bismuth NIR luminescence in bismuth-doped tantalum germanate laser glasses, Opt. Lett. 41 (7) (2016) 1340–1343.

[38] L. Su, P. Zhou, J. Yu, H. Li, L. Zheng, F. Wu, Y. Yang, Q. Yang, J. Xu, Spectroscopic properties and near-infrared broadband luminescence of Bi-doped SrB_4O_7 glasses and crystalline materials, Opt Express 17 (16) (2009) 13554–13560.

[39] Y. Qiu, J. Kang, C. Li, X. Dong, C.-L. Zhao, Broadband near-infrared luminescence in bismuth borate glasses, Laser Phys. 20 (2) (2010) 487–492.

[40] Q. Guo, B. Xu, D. Tan, J. Wang, S. Zheng, W. Jiang, J. Qiu, S. Zhou, Regulation of structure rigidity for improvement of the thermal stability of near-infrared luminescence in Bi-doped borate glasses, Opt Express 21 (23) (2013) 27835–27840.

[41] B. Denker, B. Galagan, V. Osiko, S. Sverchkov, E. Dianov, Luminescent properties of Bi-doped boro-alumino-phosphate glasses, Appl. Phys. B 87 (1) (2007) 135–137.

[42] X. Wang, Q. Sheng, L. Hu, J. Zhang, Observation of broadband infrared luminescence in a novel Bi-doped P_2O_5–B_2O_3–Al_2O_3 glass, Mater. Lett. 66 (1) (2012) 156–158.

[43] V. Dvoyrin, V. Mashinsky, E. Dianov, A. Umnikov, M. Yashkov, A. Guryanov, Absorption, fluorescence and optical amplification in MCVD bismuth-doped silica glass optical fibres, in: In 2005 31st European Conference on Optical Communication, ECOC 2005, vol. 4, IET, 2005, pp. 949–950.

[44] G. Yang, D. Chen, J. Ren, Y. Xu, H. Zeng, Y. Yang, G. Chen, Effects of melting temperature on the broadband infrared luminescence of Bi-doped and Bi/Dy co-doped chalcohalide glasses, J. Am. Ceram. Soc. 90 (11) (2007) 3670–3672.

[45] D. Guo-Ping, X. Xiu-Di, R. Jin-Jun, R. Jian, L. Xiao-Feng, Q. Jian-Rong, L. Chang-Gui, T. Hai-Zheng, Z. Xiu-Jian, Broadband infrared luminescence from bismuth-doped GeS_2-Ga_2S_3 chalcogenide glasses, Chin. Phys. Lett. 25 (5) (2008) 1891.

[46] V. Plotnichenko, D. Philippovskiy, V. Sokolov, M. Sukhanov, A. Velmuzhov, M. Churbanov, E. Dianov, Infrared luminescence in Bi-doped Ge–S and As–Ge–S chalcogenide glasses and fibers, Opt. Mater. Express 4 (2) (2014) 366–374.

[47] A.N. Romanov, E.V. Haula, Z.T. Fattakhova, A.A. Veber, V.B. Tsvetkov, D. M. Zhigunov, V.N. Korchak, V.B. Sulimov, Near-IR luminescence from subvalent bismuth species in fluoride glass, Opt. Mater. 34 (1) (2011) 155–158.

[48] E.M. Dianov, Bi-doped glass optical fibers: is it a new breakthrough in laser materials? J. Non-Cryst. Solids 355 (37–42) (2009) 1861–1864.

[49] S. Firstov, V. Khopin, I. Bufetov, E. Firstova, A. Guryanov, E. Dianov, Combined excitation-emission spectroscopy of bismuth active centers in optical fibers, Opt Express 19 (20) (2011) 19551–19561.

[50] N.K. Thipparapu, S. Jain, A. Umnikov, P. Barua, J. Sahu, 1120 nm diode-pumped Bi-doped fiber amplifier, Opt. Lett. 40 (10) (2015) 2441–2444.

[51] N. Thipparapu, Y. Wang, A. Umnikov, P. Barua, D. Richardson, J. Sahu, 40 dB gain all fiber bismuth-doped amplifier operating in the O-band, Opt Lett. 44 (9) (2019) 2248–2251.

[52] Y. Wang, N.K. Thipparapu, S. Wang, P. Barua, D. Richardson, J. Sahu, Study on the temperature dependent characteristics of O-band bismuth-doped fiber amplifier, Opt Lett. 44 (23) (2019) 5650–5653.

[53] Y. Wang, N.K. Thipparapu, D.J. Richardson, J.K. Sahu, Broadband bismuth-doped fiber amplifier with a record 115-nm bandwidth in the O and E bands,", in: 2020 Optical Fiber Communications Conference and Exhibition (OFC), 2020, pp. 1–3.

[54] Y. Wang, N.K. Thipparapu, D.J. Richardson, J.K. Sahu, Ultra-broadband bismuth-doped fiber amplifier covering a 115-nm bandwidth in the O and E bands, J. Lightwave Technol. 39 (3) (2021) 795–800.

[55] Y. Wang, N.K. Thipparapu, D.J. Richardson, J.K. Sahu, High gain Bi-doped fiber amplifier operating in the E-band with a 3-dB bandwidth of 40nm, Tu1E.1, in: Optical Fiber Communication Conference (OFC) 2021, Optica Publishing Group, 2021.

[56] S.V. Firstov, S.V. Alyshev, K.E. Riumkin, V.F. Khopin, A.N. Guryanov, M. A. Melkumov, E.M. Dianov, A 23-dB bismuth-doped optical fiber amplifier for a 1700-nm band, Sci. Rep. 6 (1) (2016) 1–6.

[57] S.R. Nagel, J.B. MacChesney, K.L. Walker, An overview of the modified chemical vapor deposition (MCVD) process and performance, IEEE Trans. Microw. Theor. Tech. 30 (4) (1979) 5676–5681.

[58] A. Khegai, S. Firstov, K. Riumkin, S. Alyshev, F. Afanasiev, A. Lobanov, A. Guryanov, M. Melkumov, Absorption cross section spectra of bismuth active centers associated with phosphorus, FM4D–3, in: Frontiers in Optics, Optica Publishing Group, 2020.

[59] A. Khegai, S. Firstov, K. Riumkin, S. Alyshev, F. Afanasiev, A. Lobanov, A. Guryanov, M. Melkumov, Radial distribution and absorption cross section of active centers in bismuth-doped phosphosilicate fibers, Opt Express 28 (20) (2020) 29335–29344.

[60] E. Desurvire, *Erbium-doped Fiber Amplifiers: Principles and Applications*, Ch. 4, Characteristics of Erbium-Doped Fibers, Wiley, 2002.

[61] W.L. Barnes, R.I. Laming, E.J. Tarbox, P. Morkel, Absorption and emission cross section of Er^{3+} doped silica fibers, IEEE J. Quant. Electron. 27 (4) (1991) 1004–1010.

[62] Rare-earth-doped fiber lasers and amplifiers, in: M.J. Digonnet (Ed.), Ch. 10, Erbium-Doped Fibere Amplifiers: Basic Physics and Characteristics, Marcel Dekker, Inc., 2001.

[63] B. Aull, H. Jenssen, Vibronic interactions in Nd:YAG resulting in nonreciprocity of absorption and stimulated emission cross sections, IEEE J. Quant. Electron. 18 (5) (1982) 925–930.

[64] N.K. Thipparapu, A. Umnikov, P. Barua, J. Sahu, Bi-doped fiber amplifier with a flat gain of 25 dB operating in the wavelength band 1320–1360 nm, Opt. Lett. 41 (7) (2016) 1518–1521.

[65] N.K. Thipparapu, Y. Wang, A.A. Umnikov, P. Barua, D.J. Richardson, J.K. Sahu, High gain Bi-doped all fiber amplifier for O-band DWDM optical fiber communication, M1J–5, in: Optical Fiber Communication Conference, Optical Society of America, 2019.

[66] A. Khegai, Y. Ososkov, S. Firstov, K. Riumkin, S. Alyshev, A. Kharakhordin, E. Firstova, F. Afanasiev, V. Khopin, A. Guryanov, et al., O-band bismuth-doped fiber amplifier with 67 nm bandwidth, W1C–4, in: Optical Fiber Communication Conference, Optical Society of America, 2020.

[67] S.V. Firstov, A.M. Khegai, A.V. Kharakhordin, S.V. Alyshev, E.G. Firstova, Y. J. Ososkov, M.A. Melkumov, L.D. Iskhakova, E.B. Evlampieva, A.S. Lobanov, M. V. Yashkov, A.N. Guryanov, Compact and efficient O-band bismuth-doped phosphosilicate fiber amplifier for fiber-optic communications, Sci. Rep. 10 (July 2020) 1–9.

[68] V. Mikhailov, J. Luo, M. Yan, G.S. Puc, Y. Sun, S.D. Shenk, D. Yuriy, R. S. Windeler, P.S. Westbrook, D. Inniss, D.J. DiGiovanni, Bismuth-doped fiber amplifiers (BDFA) to extend O-band transmission reach and capacity (Conference

Presentation), in: G. Li, X. Zhou (Eds.), Next-Generation Optical Communication: Components, Sub-systems, and Systems IX, vol. 11309, International Society for Optics and Photonics, SPIE, 2020.
[69] S. Firstov, A. Khegai, K. Riumkin, Y. Ososkov, E. Firstova, M. Melkumov, S. Alyshev, E. Evlampieva, L. Iskhakova, A. Lobanov, V. Khopin, A. Abramov, M. Yashkov, A. Guryanov, Bend-insensitive bismuth-doped P_2O_5-SiO_2 glass core fiber for a compact O-band amplifier, Opt. Lett. 45 (May 2020) 2576–2579.
[70] I.A. Bufetov, M.A. Melkumov, V.F. Khopin, S.V. Firstov, A.V. Shubin, O. I. Medvedkov, A.N. Guryanov, E.M. Dianov, Efficient bi-doped fiber lasers and amplifiers for the spectral region 1300-1500 nm, in: K. Tankala (Ed.), Fiber Lasers VII: Technology, Systems, and Applications, International Society for Optics and Photonics, SPIE, 2010, pp. 288–296.
[71] N. Taengnoi, K.R. Bottrill, N.K. Thipparapu, A.A. Umnikov, J.K. Sahu, P. Petropoulos, D.J. Richardson, WDM transmission with in-line amplification at 1.3 μm using a Bi-doped fiber amplifier, J. Lightwave Technol. 37 (8) (2019) 1826–1830.
[72] Y. Hong, K.R. Bottrill, N. Taengnoi, N.K. Thipparapu, Y. Wang, A.A. Umnikov, J. K. Sahu, D.J. Richardson, P. Petropoulos, Experimental demonstration of dual O+C-band WDM transmission over 50-km SSMF with direct detection, J. Lightwave Technol. 38 (8) (2020) 2278–2284.
[73] Y. Hong, N. Taengnoi, K.R. Bottrill, N.K. Thipparapu, Y. Wang, J.K. Sahu, D. J. Richardson, P. Petropoulos, Experimental demonstration of single-span 100-km O-band 4 × 50-Gb/s CWDM direct-detection transmission, Opt Express 30 (18) (2022) 32189–32203.
[74] S.F. Norizan, W.Y. Chong, S.W. Harun, H. Ahmad, O-Band bismuth-doped fiber amplifier with double-pass configuration, IEEE Photon. Technol. Lett. 23 (24) (2011) 1860–1862.
[75] Y. Wang, N.K. Thipparapu, A.A. Umnikov, P. Barua, D.J. Richardson, J. Sahu, Temperature dependent gain and noise figure characteristics of O-band Bismuth-doped fibre amplifier, in: 45th European Conference on Optical Communication (ECOC 2019), IET, 2019, pp. 1–3.
[76] Y. Wang, N. Thipparapu, S. Wang, P. Barua, D. Richardson, J. Sahu, O-band bismuth-doped fiber amplifier and its temperature dependent performance, in: Sixth International Workshop on Specialty Optical Fibers and Their Applications (WSOF 2019), vol. 11206, 2019, 112061X–1.
[77] E. Firstova, A. Kharakhordin, S. Alyshev, A. Khegai, M. Melkumov, S. Firstov, Depressed-cladding Bi-doped P_2O_5–SiO_2 fiber for efficient optical devices operating near 1.3 μm, SoM4H.3, in: OSA Advanced Photonics Congress (AP) 2020 (IPR, NP, NOMA, Networks, PVLED, PSC, SPPCom, SOF), Optica Publishing Group, 2020.
[78] V. Mikhailov, M.A. Melkumov, D. Inniss, A.M. Khegai, K.E. Riumkin, S.V. Firstov, F.V. Afanasiev, M.F. Yan, Y. Sun, J. Luo, G.S. Puc, S.D. Shenk, R.S. Windeler, P. S. Westbrook, R.L. Lingle, E.M. Dianov, D.J. DiGiovanni, Simple broadband bismuth doped fiber amplifier (BDFA) to extend O-band transmission reach and capacity, in: 2019 Optical Fiber Communications Conference and Exhibition (OFC), 2019, pp. 1–3.
[79] N. Taengnoi, K.R.H. Bottrill, Y. Hong, Y. Wang, N.K. Thipparapu, J.K. Sahu, P. Petropoulos, D.J. Richardson, Experimental characterization of an O-band bismuth-doped fiber amplifier, Opt Express 29 (May 2021) 15345–15355.
[80] M. Melkumov, I. Bufetov, A. Shubin, S. Firstov, V. Khopin, A. Guryanov, E. Dianov, Bismuth-doped optical fiber amplifier for 1430 nm band pumped by 1310 nm laser diode, OMH1, in: Optical Fiber Communication Conference, Optical Society of America, 2011.
[81] A. Khegai, Y. Ososkov, S. Firstov, K. Riumkin, S. Alyshev, A. Kharakhordin, V. Khopin, F. Afanasiev, A. Guryanov, M. Melkumov, Gain clamped Bi-doped fiber amplifier with 150 nm bandwidth for O-and E-bands, J. Lightwave Technol. 40 (4) (2022) 1161–1166.
[82] Y. Ososkov, A. Khegai, S. Firstov, K. Riumkin, S. Alyshev, A. Kharakhordin, A. Lobanov, A. Guryanov, M. Melkumov, Pump-efficient flattop O+E-bands bismuth-doped fiber amplifier with 116 nm 3 dB gain bandwidth, Opt Express 29 (26) (2021) 44138–44145.
[83] V. Dvoyrin, V. Mashinsky, S. Turitsyn, Bismuth-doped fiber amplifier operating in the spectrally adjacent to EDFA range of 1425-1500 nm, W1C–5, in: Optical Fiber Communication Conference, Optical Society of America, 2020.
[84] A. Donodin, V. Dvoyrin, E. Manuylovich, L. Krzczanowicz, W. Forysiak, M. Melkumov, V. Mashinsky, S. Turitsyn, Bismuth doped fibre amplifier operating in E- and S-optical bands, Opt. Mater. Express 11 (1) (2021) 127–135.
[85] A. Vakhrushev, A. Umnikov, A. Lobanov, E. Firstova, E. Evlampieva, K. Riumkin, A. Alyshev, A. Khegai, A. Guryanov, L. Iskhakova, M. Melkumov, S. Firstov, W-type and Graded-index bismuth-doped fibers for efficient lasers and amplifiers operating in E-band, Opt Express 30 (2) (2022) 1490–1498.
[86] A. Donodin, V. Dvoyrin, E. Manuylovich, M. Melkumov, V. Mashinsky, S. Turitsyn, 38 dB gain E-band bismuth-doped fiber amplifier, in: 2022 48th European Conference on Optical Communication, ECOC, 2022, p. 2022.
[87] I.A. Bufetov, S.V. Firstov, V.F. Khopin, O.I. Medvedkov, A.N. Guryanov, E. M. Dianov, Bi-doped fiber lasers and amplifiers for a spectral region of 1300–1470 nm, Opt Lett. 33 (19) (2008) 2227–2229.
[88] M. Melkumov, I. Bufetov, A. Shubin, S. Firstov, V. Khopin, A. Guryanov, E. Dianov, Laser diode pumped bismuth-doped optical fiber amplifier for 1430 nm band, Opt. Lett. 36 (13) (2011) 2408–2410.
[89] A. Khegai, Y.Z. Ososkov, S. Firstov, K. Riumkin, S. Alyshev, V. Khopin, F. Afanasiev, A. Lobanov, A. Guryanov, O. Medvedkov, et al., Wideband 26 dB bismuth-doped fiber amplifier in the range 1.3-1.44 μm, in: 2020 International Conference Laser Optics (ICLO), IEEE, 2020, 1–1.
[90] Y. Wang, N.K. Thipparapu, D.J. Richardson, J. Sahu, Bi-doped fiber amplifiers for ultra-wideband optical communication systems, in: 2021 IEEE Photonics Society Summer Topicals Meeting Series (SUM), IEEE, 2021, pp. 1–3.
[91] Y. Ososkov, A. Khegai, S. Firstov, K. Riumkin, S. Alyshev, A. Kharakhordin, A. Guryanov, A. Lobanov, M. Melkumov, Low-water-peak bismuth-doped fiber for efficient O+E band amplifiers, AW1A–3, in: Advanced Solid State Lasers, Optical Society of America, 2021.
[92] A. Khegai, Y. Ososkov, S. Firstov, K. Riumkin, S. Alyshev, A. Kharakhordin, A. Lobanov, A. Guryanov, M. Melkumov, O+E Band BDFA with flattop 116 nm gain bandwidth pumped with 250 mW at 1256 nm, Tu1E–4, in: Optical Fiber Communication Conference, Optical Society of America, 2021.
[93] F. Maes, M. Sharma, L. Wang, Z. Jiang, High power BDF/EDF hybrid amplifier providing 27 dB gain over 90 nm in the E+S band, Th4C–8, in: Optical Fiber Communication Conference, Optica Publishing Group, 2022.
[94] F. Maes, M. Sharma, L. Wang, Z. Jiang, Gain behavior of E+S band hybrid bismuth/erbium-doped fiber amplifier under different conditions, in: 2022 48th European Conference on Optical Communication, ECOC, 2022, p. 2022.
[95] A. Mansoor, N.Y.M. Omar, K.D. Dambul, H.A. Abdul-Rashid, Z. Yusoff, Optical characterisations of Bi-phosphosilicate fiber for O Band amplification, Fibers 8 (12) (2020).
[96] C.E. Max, S.S. Olivier, H.W. Friedman, J. An, K. Avicola, B.V. Beeman, H. D. Bissinger, J.M. Brase, G.V. Erbert, D.T. Gavel, et al., Image improvement from a sodium-layer laser guide star adaptive optics system, Science 277 (5332) (1997) 1649–1652.
[97] N.S. SadiCk, R. WeiSS, The utilization of a new yellow light laser (578 nm) for the treatment of class I red telangiectasia of the lower extremities, Dermatol. Surg. 28 (1) (2002) 21–25.
[98] C.F. Blodi, S.R. Russell, J.S. Pulido, J.C. Folk, Direct and feeder vessel photocoagulation of retinal angiomas with dye yellow laser, Ophthalmology 97 (6) (1990) 791–797.
[99] H. Sakr, G. Jasion, T. Bradley, Y. Chen, J. Hayes, I. Davidson, H. Mulvad, L. Xu, D. Richardson, F. Poletti, Record low loss hollow core fiber for the 1μm region, in: The European Conference on Lasers and Electro-Optics, Optical Society of America, ce_5_5, 2019.
[100] B.H. Chapman, E. Kelleher, K.M. Golant, S. Popov, J. Taylor, Amplification of picosecond pulses and gigahertz signals in bismuth-doped fiber amplifiers, Opt. Lett. 36 (8) (2011) 1446–1448.
[101] C. Crotti, F. Deloison, F. Alahyane, F. Aptel, L. Kowalczuk, J.-M. Legeais, D. A. Peyrot, M. Savoldelli, K. Plamann, Wavelength optimization in femtosecond laser corneal surgery, Investig. Ophthalmol. Vis. Sci. 54 (5) (2013) 3340–3349.
[102] F. Akhoundi, Y. Qin, N. Peyghambarian, J.K. Barton, K. Kieu, Compact fiber-based multi-photon endoscope working at 1700 nm, Biomed. Opt Express 9 (5) (2018) 2326–2335.
[103] H. Kawagoe, S. Ishida, M. Aramaki, Y. Sakakibara, E. Omoda, H. Kataura, N. Nishizawa, Development of a high power supercontinuum source in the 1.7 μm wavelength region for highly penetrative ultrahigh-resolution optical coherence tomography, Biomed. Opt Express 5 (3) (2014) 932–943.
[104] K. Wang, N.G. Horton, C. Xu, Going deep: brain imaging with multi-photon microscopy, Opt Photon. News 24 (11) (2013) 32–39.
[105] S.D. Emami, M.M. Dashtabi, H.J. Lee, A.S. Arabanian, H.A.A. Rashid, 1700 nm and 1800 nm band tunable thulium doped mode-locked fiber lasers, Sci. Rep. 7 (1) (2017) 1–8.
[106] P. Roberts, F. Couny, H. Sabert, B. Mangan, D. Williams, L. Farr, M. Mason, A. Tomlinson, T. Birks, J. Knight, et al., Ultimate low loss of hollow-core photonic crystal fibres, Opt Express 13 (1) (2005) 236–244.
[107] S.V. Firstov, S.V. Alyshev, K.E. Riumkin, A.M. Khegai, A.V. Kharakhordin, M. A. Melkumov, E.M. Dianov, Laser-active fibers doped with bismuth for a wavelength region of 1.6–1.8 μm, IEEE J. Sel. Top. Quant. Electron. 24 (5) (2018) 1–15.
[108] G. Gomółka, M. Krajewska, M. Kaleta, A.M. Khegai, S.V. Alyshev, A.S. Lobanov, S. V. Firstov, M. Nikodem, Operation of a single-frequency bismuth-doped fiber power amplifier near 1.65 μm, in: Photonics, vol. 7, Multidisciplinary Digital Publishing Institute, 2020, p. 128.
[109] K.E. Riumkin, M.A. Mel'kumov, A.V. Shubin, S.V. Firstov, I. Bufetov, V.F. Khopin, A.N. Gur'yanov, E.M. Dianov, Superfluorescent bismuth-doped fibre source, Quant. Electron. 44 (7) (2014) 700.
[110] K.E. Riumkin, M.A. Melkumov, I.A. Bufetov, A.V. Shubin, S.V. Firstov, V. F. Khopin, A.N. Guryanov, E.M. Dianov, Superfluorescent 1.44 μm bismuth-doped fiber source, Opt. Lett. 37 (23) (2012) 4817–4819.
[111] K.E. Riumkin, S.V. Firstov, S.V. Alyshev, A.M. Khegai, M.A. Melkumov, V. F. Khopin, A.V. Kharakhordin, A.N. Guryanov, E.M. Dianov, Performance of 1.73 μm superluminescent source based on bismuth-doped fiber under various temperature conditions and γ-Irradiation, J. Lightwave Technol. 35 (19) (2017) 4114–4119.